



Published in final edited form as:

Neuropharmacology. 2015 December ; 99: 242–255. doi:10.1016/j.neuropharm.2015.04.034.

An animal model of female adolescent cannabinoid exposure elicits a long-lasting deficit in presynaptic long-term plasticity

Jonathan W. Lovelace^a, Alex Corches^b, Philip A. Vieira^a, Ken Mackie^c, and Edward Korzus^{a,b,*}

^a Department of Psychology & Neuroscience Program, University of California Riverside, CA 92521, USA

^b Biomedical Sciences Program, University of California Riverside, CA 92521, USA

^c Department of Psychological & Brain Sciences, Gill Center for Biomedical Sciences, Indiana University, Bloomington, IN 47405, USA

Abstract

Cannabis continues to be the most accessible and popular illicit recreational drug. Whereas current data link adolescence cannabinoid exposure to increased risk for dependence on other drugs, depression, anxiety disorders and psychosis, the mechanism(s) underlying these adverse effects remains controversial. Here we show in a mouse model of female adolescent cannabinoid exposure a deficient endocannabinoid (eCB)-mediated signaling and presynaptic forms of long-term depression at adult central glutamatergic synapses in the prefrontal cortex. Increasing endocannabinoid levels by blockade of monoacylglycerol lipase, the primary enzyme responsible for degrading the endocannabinoid 2-arachidonoylglycerol (2-AG), with the specific inhibitor JZL184 ameliorates these deficits. The observed deficit in cortical eCB-dependent signaling may represent a neural maladaptation underlying network instability and abnormal cognitive functioning. Our study suggests that adolescent cannabinoid exposure may permanently impair brain functions, including the brain's intrinsic ability to appropriately adapt to external influences.

1. Introduction

Cannabis is the most prevalent illicit recreational drug. A total of 2.6 - 5 % of the world's population (119 - 224 million people) consume cannabis, whereas 0.3 – 0.4 % of the population consume cocaine (UNODC, 2012). On exposure to cannabis, individuals experience a variety of psychoactive effects including a general alteration of conscious perception, euphoria, impaired social interactions, disrupted memory and learning, and occasionally anxiety and paranoia. Cannabis abuse is considered to be a significant

*Correspondence should be addressed to: E.K. (edkorzus@ucr.edu).

Publisher's Disclaimer: This is a PDF file of an unedited manuscript that has been accepted for publication. As a service to our customers we are providing this early version of the manuscript. The manuscript will undergo copyediting, typesetting, and review of the resulting proof before it is published in its final citable form. Please note that during the production process errors may be discovered which could affect the content, and all legal disclaimers that apply to the journal pertain.

DISCLOSURE

The authors declare no competing financial interests.

environmental risk for neuropsychiatric disorders (Arseneault et al., 2004). It is presently accepted that many mental illnesses, including psychosis, are the result of abnormal and synergistic interactions between multiple genes and environmental factors. For example, genetic variation in the gene *COMT* is itself a well-characterized risk factor for schizophrenia (Goldberg et al., 2003). It has been demonstrated that the relative risk of developing psychosis following the use of cannabis is increased in people carrying a common polymorphism within the *COMT* (Val158Met allele) gene, but this effect was observed only in people who used cannabis during adolescence (Caspi et al., 2005). While current data link adolescent cannabis abuse to increased risk for dependence on other drugs, depression, anxiety disorders and psychosis (Arseneault et al., 2004), the mechanism(s) underlying these adverse effects remains controversial.

In the brain, cannabis exerts its psychological effects through direct binding of its active ingredient, Δ^9 -tetrahydrocannabinol (THC) (Mechoulam and Gaoni, 1965) to the G-protein-coupled, type 1-cannabinoid receptor (CB1R) (Howlett et al., 2002; Matsuda et al., 1990) expressed on presynaptic terminals (Freund et al., 2003; Gerdeman and Lovinger, 2001; Huang et al., 2001; Katona et al., 1999; Katona et al., 2006). Endogenous ligands of CB1R, which are referred as to endocannabinoids (eCBs), act as retrograde signals inhibiting neurotransmitter release (Choi and Lovinger, 1997a, b). 2-arachidonoyl glycerol (2-AG) is most abundant endogenous ligand of CB1R in the brain (Stella et al., 1997). In fact, the eCB system represents a major activity-dependent regulatory system in the central nervous system and has been implicated in multiple brain functions, including synaptic plasticity and the homeostatic regulation of network activity patterns (Freund et al., 2003; Gerdeman and Lovinger, 2003; Piomelli, 2003; Raver et al., 2013; Sales-Carbonell et al., 2013). CB1R-mediated decreased probability of neurotransmitter release underlies transient, depolarization-induced synaptic inhibition (Wilson and Nicoll, 2001), long-term depression (Choi and Lovinger, 1997b) and the postnatal development of corticostriatal synapses (Choi and Lovinger, 1997b).

During adolescence, the prefrontal cortex (PFC), one of the latest regions of the brain to mature, undergoes significant developmental modification of its circuits that can be translated to cognitive, emotional and behavioral progression (Gogtay et al., 2004). Although the behavioral effects of administration of CB1R agonists during adolescence have been studied (Raver et al., 2013; Realini et al., 2011; Rubino et al., 2009; Rubino et al., 2008; Zamberletti et al., 2014), the possible permanent effects of CB1R hyperactivity during adolescence on mPFC network physiology are still unclear. Studies of adult female rats exposed to THC during adolescence revealed altered behaviors including anhedonia, behavioral despair, reduced sociability, deficits in spatial-working and object recognition memory, as well as sensitization to phencyclidine locomotor-activating effects (Realini et al., 2011; Rubino et al., 2009; Rubino et al., 2008; Zamberletti et al., 2014). Similarly treated male rats also developed abnormal behavior in adulthood but behavioral changes were less complex and limited to cognitive deficits (Rubino et al., 2009; Rubino et al., 2008). In addition, exposure to cannabinoids during adulthood was ineffective in producing this phenotype in female rats (Realini et al., 2011).

To detect potential prefrontal maladaptations triggered by adolescent cannabinoid exposure, we tested multiple forms of presynaptic plasticity at glutamatergic synapses in cortical layers 2/3 to 5 (L2/3->L5) in the mPFC of adult female mice treated sub-chronically during adolescence with the cannabinoid agonist, WIN55,212-2 and investigated the effects of this treatment on presynaptic plasticity in the adult. We found that two types of long-term depression (LTD), LTD mediated by metabotropic glutamate receptors 2/3 (mGluR2/3) and LTD mediated by CB1Rs, were deficient in adulthood in mice treated with WIN55,212-2. Over-activation of the CB1R during adolescence could therefore lead to permanent developmental changes in the expression of presynaptic LTD in the mPFC at excitatory synapses. These observations could be linked to a maladaptation of the mPFC network during a critical period of cortical development and may underlie the alteration of gamma oscillations in adults after adolescent CB1R stimulation, as found in earlier studies (Raver et al., 2013; Sales-Carbonell et al., 2013; Skosnik et al., 2012).

2. Methods

2.1. Subjects

C57BL/6 mice were used for all of the experiments following protocols approved by the IACUC at University of California Riverside. The animals were housed in plastic cages (2-4 mice/cage) and kept on 12/12 h dark/light cycle with ad libitum access to food and water. Ten- to twenty-four-week-old mice were used for the physiological studies. To generate the WIN-55,212-2 treated animals, C57BL/6 mice were intraperitoneally injected twice a day with increasing doses of (+)WIN55, 212-2 (mesylate), once in the morning and once in the afternoon at the same times of day on postnatal days (PND) 35-45 as in previous studies (Rubino et al., 2008). All of the physiological tests were performed using only females during adulthood (P70-P170).

2.2. Drugs - physiology

WIN55,212-2 was obtained from NIMH Chemical Synthesis and Drug Supply Program. Picrotoxin, 6,7-dinitroquinoxaline-2,3-dione (DNQX), LY379268, JZL 184, and AM 251 were obtained from Tocris, Inc. All drugs used in electrophysiological procedures were made from stock solutions and frozen in aliquots at -20°C until used on day of the experiment. For bath application in physiological studies, WIN55,212-2, JZL 184, AM 251, and picrotoxin were dissolved in DMSO and made into 100mM stock solutions. LY379268 was dissolved in water and stored in 10mM stock solutions. The concentration of DMSO was always <0.1% of total concentration and had no effect on synaptic responses. All experiments were done in the presence of 50µM picrotoxin in order to block ionotropic GABA mediated transmission unless stated otherwise.

2.3. Drugs – animal injection

The WIN55,212-2 injection solution was prepared using a mixture of EtOH / Cremophor / saline in a 1:1:18 ratio (Acheson et al., 2011; López-Gallardo et al., 2012). Stock solutions of WIN55, 212-2 were stored in the same volume of ethanol in varying dilutions for use on different days to achieve the appropriate dose. On the day of injection, WIN55,212-2 stock solution was mixed with cremophor and saline, vortexed, and brought to room temperature

before injection. Mice received I.P. injections twice a day at the same time of day on days PND 35-45 as previously described; low doses were at 0.5 mg/kg (PND 35-36), medium doses at 1 mg/kg (PND 37-41), and high doses at 2 mg/kg (PND 42-45) (Figure 1A).

2.4. Electrophysiology

Local field postsynaptic potential (fPSP) recordings were obtained from cortical layer 5 in the prelimbic (PL) region of the mPFC after stimulation at layer 2/3 inputs. Acute brain slices containing the mPFC were prepared using the Compresstome VF-300 (Precisionary Instruments, Greenville, NC). Ex vivo slice electrophysiology was performed on brain slices containing the PL region of the mPFC bathed in ACSF (124.00 mM NaCl, 4.40 mM KCl, 25.00 mM NaHCO₃, 1.2 mM Na₂HPO₄, 1.3 mM MgSO₄·7H₂O, 2.5 mM CaCl₂·2H₂O, and 10 mM glucose) saturated with a 95% O₂/5% CO₂ gas mixture. Brain slices containing the PL region were placed in a recording chamber and continuously perfused [~1.5 ml/min] with carboxygenated ACSF held at 28°C. The slices were viewed under an Olympus TM FV1000 confocal microscope using DIC. In all cases, local field potential recordings were obtained from cortical layer 5 in the PL region using a 1.5-5 MΩ resistance glass pipette filled with ACSF and guided by visual landmarks combined with adjustment for the maximal fPSP response within a region ~500-800 μm from the cortical surface. Signals from the head stage were then amplified, filtered, digitized at 10 KHz, and sent to a computer for data storage using Clampex software and analyzed using Clampfit (Molecular Devices Inc.). Stimulations were delivered using a bipolar cluster electrode (FHC, Inc.) placed in cortical layers 2/3 in the PL region of the mPFC, which was visible under DIC as a dark band ~200-300 μm from the surface. The stimulating electrode was aligned with the recording electrode, which was perpendicular to the cortical surface.

Acute mPFC slices from 10- to 24-week-old mice were used for recordings, which were performed according to previously described protocols: input/output (I/O) and paired-pulse ratio (PPR) (Limback-Stokin et al., 2004), short-term potentiation (STP) (Hempel et al., 2000), endocannabinoid-dependent LTD (eCB-LTD) (Lafourcade et al., 2007), and mGlu_{2/3} LTD (Kasanetz et al., 2013). The glutamatergic nature of the fEPSP was confirmed by blocking it with 20 mM DNQX (AMPA receptor antagonist) (no picrotoxin present). Traces from the local field potential recordings were analyzed as previously described (Hempel et al., 2000; Hirsch and Crepel, 1990; Morris et al., 1999). The I/O was recorded starting at 20 μA stimulation using an isolated stimulator, and the stimulation intensity was then increased until the amplitude measurements reached a plateau (three consecutive stimulus intensity increases with minimal change). The individual curves were fitted using Boltzmann's sigmoidal fit equation: $y = [A2 + (A1-A2)]/[1 + \exp((x-x_0)/dx)]$ and OriginPro software (OriginLab, Inc.). An R-square value of >0.9 was used as a cut-off criterion for curve fitting. PPR was used to assess the transient synaptic plasticity at increasing interstimulus intervals (ISI) ranging from 25 ms to 300 ms tested at both 30% and 70% of the stimulation required to reach maximum (no picrotoxin present). The PPR and I/O stimulation were determined by the average of three traces with 15 s intervals between stimulations.

STP was induced using a 15-pulse 50 Hz train with at least 20 min of post-stimulus train recording (no picrotoxin present). The test pulses were delivered every 10 s. The STP was measured at 30% and 70% of the stimulation intensity needed to reach maximum. Post-train recordings were compared to baseline recordings as a percentage of the average baseline for amplitude of fPSP. eCB-LTD was induced according to a previously published protocol (Lafourcade et al., 2007) in which a 10-min, 10-Hz stimulation (at 70% stimulus intensity) of layer 2/3 in the PL region of the mPFC induced long-lasting LTD in layer 5 pyramidal neurons. Long-lasting LTD was then recorded for 1 hr, with test pulses delivered at a rate of 0.1Hz. mGluR2/3-LTD was induced at time 0 with a 10-minute bath application of 100 nM LY379268 (a potent mGluR2/3 agonist). The success or failure of LTD expression in individual groups was determined using a paired Wilcoxon signed rank test (Wilcoxon test) by comparing the mean fPSP amplitude during baseline (10 min before stimulation) and 50-60 min after LTD induction. When recording during mGluR2/3-LTD and WIN55,212-2 application, test pulses were delivered at a rate of 0.1 Hz with at least 20 min of baseline recording before drug application.

2.5. Novel Object Recognition

Novel Object Recognition (NOR) was performed as previously described (Korzus et al., 2004). The task is divided into four phases: habituation, familiarization, delay and test. 1) Mice were handled 4 times and were placed in the experimental room for two hours before the experiment. 2) During familiarization two identical objects were placed in the home cage with the animals for 5 min. 3) Animals were tested after a 5 min. delay. 4) During the test phase both the familiar object (a replica of the original familiar object was used to avoid the use of odor cues) and a novel object were placed in the cage. Object exploration times (for both familiar and novel objects) were recorded for a 2 min test period. We employed computer-assisted scoring using software to measure time spent exploring an object and analyze performance on the NOR task. Observer-assessed object exploration was scored using computer interface when the animal's head was oriented towards the object and vibrissae were moving. The objects varied in color, shape and size and were balanced so that the same objects (replicas) were used for some animals as "familiar" and for others as "novel" in the same session. Also the position of "novel" and "familiar" objects within the cage was randomized.

2.6 Open Field Activity

Anxiety-related behavioral responses and locomotor activity were scored and analyzed using an Open Field Activity test performed in novel environment following protocols described before (Korzus et al., 2004). A 17" × 17" × 12" clear Plexiglas arena with a white acrylic floor was used for the open field test. The arena was located in a sound attenuated chamber with lights and a ceiling mounted camera. After sanitizing the arena with Quatricide TB, 70%EtOH, and distilled water, mice were individually placed inside and allowed to explore for 10 min before being returned to their home cage. Videos were analyzed offline using behavioral analysis software Ethowatcher (Crispim Junior et al., 2012) to measure indices of anxiety and locomotion.

2.7. Histology

Brains isolated from transcardially perfused mice with 4% PFA were additionally fixed by overnight incubation 4% PFA at 4°C and then transferred to Phosphate Buffered Saline solution, pH 7.4 (PBS) with 0.02% NaN₂. 50 µm brain slices including prefrontal cortex (prepared using a Leica Cryostat) were placed in 24-well plates for free floating immunocytochemistry (IHC). Sections are washed 3 times for 10 min in a Washing Buffer (PBS, 0.3% Triton x-100, 0.02% NaN₃) before 1 h incubation in Blocking Buffer (5% normal goat serum in washing buffer) followed by 10 min incubation in the Washing Buffer. Slices were incubated overnight at 4°C with primary antibodies (rabbit anti-CB1R IgG, CB1-L15 (Bodor et al., 2005) or rabbit anti-mGluR2/3 IgG from Millipore or rabbit anti-MAGL, IgG (Straiker et al., 2009) 1:1000 and guinea pig anti-vGlut1 IgG from Synaptic Systems, 1:1000) in the Blocking Buffer. After three washes with the Washing Buffer, slices were incubated with secondary antibodies (Alexa647-donkey anti-rabbit IgG; Molecular Probes, 1:1000 and Alexa555-goat anti guinea pig IgG, Molecular Probes, 1:1000) in the Blocking Buffer overnight at 4°C. Slices were washed again 3 times with the Washing Buffer before mounting for viewing. Immuno-stained tissue was analyzed on a semi-automatic laser scanning confocal microscope Olympus FV1000 controlled by Fluoview software. Fluorescence was measured from mPFC slices using objective 40x/0.80 LUMPlanFL40x objective. A single optical section was taken from the cortical layer 5 of the PL region in the mPFC at 10 µm below the surface and used for analysis. Average intensity of each channel across the entire 800x600 ROI collected at was used as our measure of signal intensity in the mPFC. Gain and offset of each channel were balanced manually using Fluoview saturation tools for maximal contrast. All settings were tested on multiple slices before data collection and brain slices were imaged using identical microscope settings once established. The background fluorescence for each channel using established image acquisition settings was measured in negative control experiments for each group (secondary without primary) and subtracted from final image calculations. Pixel-based image analysis including the fluorescence intensity quantification and fluorescence signal overlap between channels for colocalization analysis were performed on original images by the use of Olympus Fluoview software without any non-linear image adjustments.

2.8. Data analysis

Experimenters were blind to group designations. Data represent means ± SEM. Statistical analysis was performed using Excel (Microsoft, Inc.) or SPSS (IBM, Inc.). Student's *t* test, Wilcoxon signed ranked test or repeated measures ANOVA (RM-ANOVA) was used for statistical comparisons. In cases where RM-ANOVA was utilized and assumptions of sphericity were violated (via Mauchly's Test), analysis was completed using the Greenhouse-Geisser correction. A critical probability of $p = 0.05$ was applied. Asterisks indicate statistical significance: *, $p < 0.05$; **, $p < 0.01$; ***, $p < 0.001$.

3. Results

3.1. Adolescent WIN55 exposure triggers a deficit in eCB-dependent LTD in the mPFC

To test the hypothesis that elevated levels of cannabinoids during adolescence trigger lasting abnormalities in neural network functioning, we exposed mice to repeated doses of the

CB1R agonist WIN55,212-2 (WIN55-treated mice) or vehicle (control, CTRL) during adolescence as described in methods (Figure 1A) and tested synaptic activity at the L2/3→L5 glutamatergic synapses (Hempel et al., 2000; Morris et al., 1999) (Figure 1B). These cortical glutamatergic synapses (Figure 1C) represent one of the major pathways in the mPFC because convergent cortical and subcortical pathways are integrated in cortical layer L2/3 pyramidal neurons, which form abundant contacts with pyramidal neurons in cortical layer L5, from which the output of the cortex originates.

One way to capture how a synapse transforms signals is to analyze the relationship between its input and its output (*I/O*). Analysis of the shape of the *I/O* curve may provide valuable information about additive operations (shift along the input axis) or gain (slope change). *I/O* relations appear to be similar in WIN55-treated and control mice (Figure 1D; main effect of group, $F_{(1,146)} = 0.425$, $p = 0.5156$; Group \times Intensity $F_{(7,146)} = 0.146$, $p = 0.9942$). Additional detailed analysis of the *I/O* relationship was performed to determine whether differences in the shape of the curves existed using different metrics obtained from Boltzmann sigmoidal analysis. Comparison of the means of individual Boltzmann-fitted parameters revealed no differences between WIN55-treated and control mice in maximum asymptote (A2: CTRL: 0.85 ± 0.08 mV, $n = 10$; WIN55-treated, 0.82 ± 0.13 mV, $n = 11$; $t_{(19)} = 0.1107$, $p = 0.9130$), in the center (x_0 : CTRL: 56.86 ± 5.88 μ A, $n = 10$; WIN55-treated: 71.83 ± 8.37 μ A, $n = 11$; $t_{(19)} = 1.4347$, $p = 0.1676$), or in the time constant (dx : CTRL: 21.34 ± 2.39 , $n = 10$; WIN55-treated: 20.38 ± 3.16 , $n = 11$; $t_{(19)} = 0.2390$, $p = 0.8137$). These observations suggest that there are no differences in any of the tested characteristics of the *I/O* curves. Thus, by these measures, WIN55-treated mice showed unaltered synaptic transmission in the L2/3→L5 pathway, indicating that synaptic density within the population was normal and that synaptic transmission was equally effective in response to a single stimulus following WIN55 treatment.

eCB-LTD is a widespread form of cortical plasticity that provides activity-dependent inhibitory control of neurotransmitter release. The CB1R is required for the induction of eCB-LTD (Figure 1E). eCB-LTD is also a presynaptic form of plasticity that is negatively coupled to the cAMP/PKA signaling pathway via $G_{i/o}$ (Lovinger, 2008b). We used a moderate stimulation protocol of 10 Hz for 10 min at 70% stimulus intensity to induce eCB-LTD at L2/3→L5 glutamatergic synapses in the mPFC (Figure 1F); this protocol has been shown to produce long-term depressive effects that persist for at least 1 hour (Lafourcade et al., 2007). The success or failure of LTD expression in individual groups was determined using a paired Wilcoxon signed rank test (Wilcoxon test) by comparing the mean fPSP amplitude at baseline (10 min before stimulation) and 50-60 min after LTD induction. Comparative analysis of the mean fPSP amplitude at baseline and 50-60 min after LTD induction revealed robust LTD expression in control animals (Figure 1F, Wilcoxon test: $55.82\% \pm 4.08\%$, $Z = -2.201$, $n = 6$, $p = 0.028$). It is well established that the expression of LTD induced by application of a 10-Hz train to the mPFC for 10 min is coupled to CB1R (Lafourcade et al., 2007; Lovelace et al., 2014; Lovinger, 2008b). Not surprisingly, bath application of CB1R inhibitors such as AM 251 blocked the induction of eCB-LTD in the L2/3→L5 pathway in acute brain slices isolated from control animals (Figure 1E, Wilcoxon test: AM 251: $101.18\% \pm 6.48\%$, $Z = 0$, $n = 4$, $p = 1.00$). Comparative analysis of the last 10

min of recordings (Figure 1E) revealed differences between control and AM 251-treated slices (CTRL: $55.82\% \pm 4.08\%$, $n = 6$; AM 251: $101.18\% \pm 6.48\%$, $n = 4$; $t_{(8)} = -6.274$, $p = 0.0002$). Then, we examined eCB-LTD in the L2/3→L5 pathway in WIN55-treated mice. The WIN55-treated mice showed a marked deficit in eCB-LTD induction in the L2/3→L5 pathway in the mPFC (Figure 1F, Wilcoxon test: $90.54\% \pm 7.63\%$, $Z = -1.125$, $n = 9$, $p = 0.260$). Thus, mice exposed to this cannabinoid during adolescence show a strong deficit in eCB-LTD but not in baseline synaptic transmission.

3.2. Short-term plasticity is unaffected in WIN55-treated mice

To examine the effects of WIN55 administration during a critical time for maturation of plasticity in the PFC circuit, we tested short-term plasticity in the L2/3→L5 pathway in the mPFC from adult WIN55-treated mice. Multiple forms of short-term plasticity can be expressed at L2/3→L5 excitatory synapses, including the paired-pulse ratio of peak amplitudes (PPR), short-term potentiation (STP) and short-term depression (STD) (Hempel et al., 2000; Morris et al., 1999).

PPR were measured at the L2/3→L5 synapse at 5 different interstimulus intervals (25, 50, 100, 200, and 300 ms) using 30% stimulus intensity (Figure 2A). No differences in mean PPR were observed between CTRL ($n = 6$) and WIN55-treated ($n = 10$) animals at 25 ms (CTRL = $180.87\% \pm 29.08\%$; WIN55-treated = $167.457\% \pm 9.98\%$; $t_{(14)} = 0.5248$, $p = 0.6079$), 50 ms (CTRL = $196.10\% \pm 28.20\%$; WIN55-treated = $185.22\% \pm 14.22\%$; $t_{(14)} = 0.3844$, $p = 0.7065$), 100 ms (CTRL = $191.09\% \pm 16.05\%$; WIN55-treated = $185.43\% \pm 14.35\%$; $t_{(14)} = 0.2531$, $p = 0.8039$), 200 ms (CTRL = $138.44\% \pm 11.89\%$; WIN55-treated = $144.80\% \pm 8.58\%$; $t_{(14)} = 0.4421$, $p = 0.6652$), or 300 ms (CTRL = $124.31\% \pm 14.23\%$; WIN55-treated = $126.16\% \pm 8.33\%$; $t_{(14)} = 0.1208$, $p = 0.9056$) (Figure 2A).

Short-term potentiation (STP) was induced by a brief train of 15 pulses delivered at a rate of 50 Hz at time 0 (Figure 2B). Test pulses were delivered at a rate of 0.1Hz using 30% of maximum stimulation as determined by individual fitted I/O curves. RM-ANOVA between WIN55-treated ($n = 9$) and CTRL ($n = 6$) animals was conducted on 6 binned time points between 0 and 600 s (100 s bins). No time \times treatment interaction was found ($F_{(1.6, 21.3)} = 1.568$, $p = 0.232$) (Figure 2B). Short-term depression (STD) was measured during the train used to simulate STP. Each response in the train was compared to the fPSP amplitude at baseline and plotted as a percentage of that value. Depression across the train was observed in all groups, with facilitation being favored in the early portion of the train (Figure 2C). RM-ANOVA using 5 binned data points (3 pulse bins) revealed no significant pulse# \times treatment interaction ($F_{(2.1, 28.7)} = 0.284$, $p = 0.760$).

We also measured forms of short-term plasticity at 70% stimulus intensity under the same conditions used to test LTD. Thus, PPRs were measured at 70% stimulus intensity using the same ISIs as those shown in Figure 2A (Figure 2D). No differences were observed between CTRL ($n=6$) and WIN55-treated ($n=10$) animals based on independent samples t-tests at 25 ms (CTRL = $125.23\% \pm 15.29\%$; WIN55-treated = $131.63\% \pm 9.45\%$; $t_{(14)} = 0.3780$, $p = 0.7111$), 50 ms (CTRL = $126.54\% \pm 9.60\%$; WIN55-treated = $134.29\% \pm 8.37\%$; $t_{(14)} = 0.5896$, $p = 0.5648$), 100 ms (CTRL = $124.97\% \pm 9.60\%$; WIN55-treated = $134.25\% \pm 4.94\%$; $t_{(14)} = 0.9546$, $p = 0.3560$), 200 ms (CTRL = $116.22\% \pm 8.26\%$; WIN55-treated =

121.69% \pm 6.38%; $t(14) = 0.5245$, $p = 0.6081$), or 300 ms (CTRL = 114.04% \pm 7.21%; WIN55 = 113.29% \pm 6.09%; $t(14) = 0.0777$, $p = 0.9392$).

RM-ANOVA on STP at the 70% stimulus intensity between WIN55-treated ($n=10$) and CTRL ($n=6$) was also conducted on 6 binned time points between 0 and 600 s (100 s bins). No time \times treatment interaction was observed at 70% stimulus intensity ($F_{(2.1, 29.5)} = 1.501$, $p = 0.239$) (Figure 2E).

STD at 70% stimulus intensity was also measured (Figure 2F). Depression across the train was observed in all groups, with facilitation being favored in the early portion of the train, but to a lesser extent than at 30% stimulus intensity. RM-ANOVA using 5 binned data points (3 pulse bins) revealed no significant pulse# \times treatment interaction $F_{(4,56)} = 2.154$, $p = 0.086$ (Figure 2F). Taken together, these results suggest that basic communication and short-term plasticity at L2/3 \rightarrow L5 glutamatergic excitatory synapses in WIN55-treated mice are unaffected by WIN55 treatment during adolescence.

3.3. Inhibition of 2-AG hydrolysis ameliorates the eCB-LTD deficiency at L2/3 \rightarrow L5 synapses

Treatment of adolescent mice with WIN55 induced a long-lasting deficit in eCB-LTD expression when compared with control animals (Figure 3A, CTRL: 55.82% \pm 4.08%, $n = 6$; WIN55-treated: 90.54% \pm 7.63%, $n = 9$; $t_{(13)} = 3.469$, $p = 0.004$). However, inhibition of monoacylglycerol lipase (MAGL), the primary enzyme responsible for degrading the endocannabinoid 2-arachidonoylglycerol (2-AG) (Makara et al., 2005), with the specific inhibitor JZL 184 (Long et al., 2009) ameliorated the eCB-LTD deficit in the WIN55-treated mice (Figure 3A-B, Wilcoxon test for WIN55-treated+JZL 184: 69.46% \pm 4.90%, $Z = -2.366$, $n = 7$, $p = 0.018$). The level of expression of eCB-LTD also differed significantly from that observed in brain slices from WIN55-treated animals without bath application of JZL 184: WIN55-treated+JZL 184 vs. WIN55-treated: $t(14) = 2.170$, $p = 0.048$).

The eCB-LTD has been studied before at the L2/3 \rightarrow L5 synapse in the mPFC and there is a good body of evidence eCB-LTD at the L2/3 \rightarrow L5 synapse in the mPFC in mice depends on eCB system (Jung et al., 2012; Lafourcade et al., 2007; Lovelace et al., 2014; Thomazeau et al., 2014). It was also demonstrated that 2-AG degradation is a critical limiting factor for eCB-LTD and blocking anandamide (a second endocannabinoid) degradation has no effect on eCB-LTD expression (Lafourcade et al., 2007)(Marrs et al., 2010). However, there is also a possibility for unknown compensatory adaptations in non-CB1R receptors in a mutant or pharmacologically treated animal model such as WIN55-treated mice. Thus, we have also tested if the JZL 184 mediated rescue of impaired eCB-LTD in WIN55-treated mice depend on the function of CB1Rs. Data in Figure 1A-B show that the attempt to rescue impaired eCB-LTD with JZL 184 in the presence of selective blocker of CB1R function (AM 251) failed (Figure 3A-B; Wilcoxon test for WIN55-treated - JZL 184 +AM 251: 90.42% \pm 0.045, $Z = -1.572$, $n=6$, $p = 0.116$). In fact, the levels of eCB-LTD expression were not different from that observed in brain slices from WIN55-treated animals without bath application of JZL 184 and AM 251 (WIN55 - ACSF compared to WIN55 - JZL 184+AM 251: $t(13) = 0.032$, $p = 0.975$) but differed significantly from that observed in brain slices from WIN55-treated animals with bath application of JZL 184 alone (WIN55 - JZL

184+AM 251 compared to WIN55 – JZL 184: $t(11) = 3.079$, $p = 0.010$). Together, these results strongly suggest that the eCB system is disrupted in WIN55-treated mice and can be rescued by increasing 2-AG levels, but only in presence of functional CB1Rs.

3.4. Adolescent WIN55 exposure reduces CB1R functionality in the mPFC

Induction of eCB-LTD at L2/3→L5 synapse in the mPFC can be effectively abolished by the direct inhibition of CB1R function (Figure 1E), a finding that is consistent with previous reports (Lafourcade et al., 2007). It is possible that the observed deficits in eCB-LTD result from the development of abnormal CB1R-dependent signaling in WIN55-treated animals as a compensatory mechanism within the mPFC network. We measured the direct responsiveness of CB1R to its well-characterized agonist WIN55,212-2 using an acute brain slice preparation in WIN55-treated and control animals. Evoked fPSPs in L5 stimulated at the L2/3 inputs in the mPFC were strongly inhibited by bath perfusion of control slices with 1 μ M WIN55,212-2 (Figure 3C-D), whereas slices from WIN55-treated mice showed a modest reduction in response (Figure 3D, RM-ANOVA: time \times treatment: $F_{(1.8, 17.5)} = 9.254$, $p = 0.0024$).

3.5. Adolescent WIN55 exposure attenuates mGluR2/3-dependent LTD

Activation of mGluR2/3 receptors is known to induce LTD (mGluR2/3-LTD) in the PFC with a presynaptic locus of expression (Robbe et al., 2002) and can compensate for deficiencies in eCB-LTD following chronic THC treatment (Mato et al., 2004). We examined mGluR2/3-LTD in WIN55-treated mice at the L2/3→L5 pathway. Figure 4 shows that the mGluR2/3 agonist LY379268 was effective in inducing robust mGluR2/3-LTD in both control and WIN55-treated mice (Figure 4A-B; Wilcoxon test: CTRL: $59.85\% \pm 3.58\%$, $Z = -2.201$, $n = 6$, $p = 0.028$; WIN55-treated: $76.62\% \pm 2.06\%$, $Z = -2.521$, $n = 8$, $p = 0.012$). However, the level of expression of mGluR2/3-LTD was greater in control mice compared to WIN55-treated mice (Figure 4C, RM-ANOVA: time \times treatment: $F_{(6,72)} = 3.715$, $p = 0.003$), indicating that mechanisms controlling presynaptic mGluR2/3-LTD, including those shared with eCB-LTD, are impaired in WIN55-treated mice. Additional comparison of the last 10 minutes of recording showed a significant difference in the final level of mGluR2/3 depression in WIN55-treated mice and controls (Figure 4D; CTRL: $59.61\% \pm 3.27\%$, $n = 6$; WIN55-treated: $76.62\% \pm 2.06\%$, $n = 8$; $t_{(12)} = 4.625$, $p = 0.001$). These results show that WIN55-treated mice still express mGluR2/3 LTD but that the magnitude of the LTD is suppressed in WIN55-treated mice compared to that of controls. Thus, both forms of presynaptic plasticity, mGluR2/3-LTD and eCB-LTD, are impaired in this mouse model of adolescent cannabinoid exposure.

3.6. Adolescent WIN55 exposure alters the expression of proteins relevant to presynaptic plasticity at glutamatergic synapses in the mPFC.

Figure 1F and 4B demonstrate presence of deficits in two forms of presynaptic plasticity (i.e. eCB-LTD and mGluR2/3-LTD, respectively) at glutamatergic L2/3→L5 synapses in the mPFC after exposure to a cannabinoid during adolescence. Previous studies demonstrated that CB1R and mGluR2 proteins show highly overlapped expression patterns in cortical layer 5 of the mPFC {Mato, 2005 #5976}. We wanted to determine if the observed deficits in these forms of plasticity could be due to alterations in the expression of proteins relevant

for the glutamatergic synapse maturation and function. Thus, we examined the levels and distribution of CB1R, mGluR2/3, MAGL and the vesicular glutamate transporter type-1 (VGluT1) in cortical layer 5 of the PL mPFC in WIN55-treated mice using immunohistochemistry (Figure 5). While total CB1R protein levels in WIN55 mice weren't significantly different (Figure 5A, CTRL: 1 ± 0.165 , $n=9$; WIN55: 0.69 ± 0.048 , $n=12$; $t_{(19)} = 2.0211$, $p = 0.0576$) perhaps due to the high level of CB1R expression on inhibitory terminals (see below), total mGluR2/3 levels in WIN55-treated animals showed a modest decrease in the mPFC (Figure 5B, CTRL: 1 ± 0.137 , $n=12$; WIN55: 0.657 ± 0.051 , $n=10$; $t_{(20)} = 2.176$, $p = 0.0417$). Total levels of MAGL (Figure 5C, CTRL: 1 ± 0.07 , $n=12$; WIN55: 1.01 ± 0.15 , $n=11$; $t_{(21)} = 0.044$, $p = 0.965$) in WIN55-treated mice were not different from those found in control animals. In addition, WIN55-treated mice did not show any changes in total levels of expression of VGluT1 (Figure 5D, CTRL: 1 ± 0.07 , $n=33$; WIN55: 0.98 ± 0.11 , $n=33$; $t_{(64)} = 0.177$, $p = 0.860$), which marks glutamatergic terminals from neurons residing in cortical regions (Fremeau et al., 2004a; Fremeau et al., 2004b).

Induction of eCB-LTD can be blocked via the direct inhibition of CB1R function (Figure 1E), which is consistent with previous reports, e.g. (Lovinger, 2008a). While there was obvious deficit in eCB-LTD expression at the L2/3→L5 excitatory synapse of the PL mPFC in WIN55-treated mice, the difference between the WIN55-treated and control mice in CB1R protein level fell short of statistical significance (Figure 5A, $p = 0.0576$). Previous immunocytochemical studies revealed that CB1Rs receptors are mainly present on the plasma membranes of axons and axon terminals (Nyiri et al., 2005) of both inhibitory and excitatory neurons in the brain (Harkany et al., 2008; Mackie, 2008). Thus we have analyzed co-localization of CB1R in L5 of the PL mPFC with VGluT1, which marks glutamatergic terminals (Fremeau et al., 2004a; Fremeau et al., 2004b). High-resolution confocal laser scanning microscopy revealed that the CB1R expression pattern resembles fibers and punctate-like structures reminiscent of axons and axonal terminal (Figure 5E), which is consistent with previous studies (Katona et al., 1999; Tsou et al., 1999). VGluT1 positive terminals were found to co-localize with CB1R immunoreactivity in L5 of the PL mPFC at a low frequency. WIN55-treated animals showed a decrease in co-localization of CB1R with vGluT1 in L5 in PL of the mPFC (Figure 5E, CTRL: 1 ± 0.5 , $n=9$; WIN55-treated: 0.62 ± 0.073 , $n=12$; $t_{(19)} = 2.2698$, $p = 0.0351$). These data suggest that adolescent exposure to cannabinoid disrupts signaling by altering the distribution/levels of major mediators of presynaptic plasticity, such as CB1R and mGluR2/3, at glutamatergic synapse in the mPFC.

3.7. Adolescent WIN55 exposure triggers cognitive deficiency

To test the hypothesis that adolescent WIN55 exposure leads to a permanent deficit in performance on cognitive tasks, we examined WIN55-treated mice in a novel object recognition test that is sensitive to decreased working memory, a cognitive behavior consistently impaired in schizophrenic patients (Forbes et al., 2009). Consistent with a previous report (Raver et al., 2013), WIN55-treated mice exhibited abnormal behavior in the novel object recognition task (Figure 6A-B). The total time spent exploring both objects was the same in WIN55-treated and control mice during training (Figure 6A, CTRL: $64.92 \text{ s} \pm 10.05 \text{ s}$, $n=10$; WIN55-treated: $63.17 \text{ s} \pm 4.22 \text{ s}$, $n=6$; $t_{(14)} = 0.1292$, $p = 0.8991$) and

testing (Figure 6A, CTRL: $32.36 \text{ s} \pm 3.64 \text{ s}$, $n = 10$; WIN55-treated: $28.12 \text{ s} \pm 1.98 \text{ s}$, $n = 6$; $t_{(14)} = 0.8499$, $p = 0.4097$).

The two groups of mice showed no difference in discrimination between objects during training (Figure 6B, CTRL: -0.11 ± 0.05 , $n = 10$; WIN55-treated: -0.05 ± 0.028 , $n = 6$; $t_{(14)} = 0.8072$, $p = 0.4330$). However, whereas control mice displayed a strong bias towards the novel object during the test, WIN55-treated mice were not able to learn to discriminate between the familiar and the novel object (Figure 6B, CTRL: 0.398 ± 0.066 , $n = 10$; WIN55-treated: 0.0482 ± 0.085 , $n = 6$; $t_{(14)} = 3.2658$, $p = 0.0056$).

In addition, WIN55-treated mice showed normal levels of locomotor activity (Figure. 2C-D. Total Distance Traveled: CTRL: $28.44\text{m} \pm 3.88\text{m}$, $n = 10$; WIN55: $34.82\text{m} \pm 1.25\text{m}$, $n = 14$; $t_{(22)} = 1.2356$, $p = 0.2297$. Average Velocity: CTRL: $5.21\text{cm/s} \pm 0.48\text{cm/s}$, $n = 10$; WIN55: $5.81\text{cm/s} \pm 0.21\text{cm/s}$, $n = 14$; $t_{(22)} = 1.2283$, $p = 0.2323$) and moderate deficit in anxiety-related responses (Figure 6E, CTRL: $6.13\% \pm 0.78\%$, $n = 10$; WIN55: $10.59\% \pm 0.94\%$, $n = 14$; $t_{(22)} = 3.4246$, $p = 0.0024$).

4. Discussion

During adolescence, extensive maturation of prefrontal circuits coincides with profound changes in behavior and cognitive abilities. Human studies have shown that cannabis abuse during adolescence can increase the risk of psychiatric disorders later in adulthood (Arseneault et al., 2004; Fernandez-Espejo et al., 2009; Luzi et al., 2008; Manrique-Garcia et al., 2011; Rubino et al., 2011; Ujike and Morita, 2004). The importance of eCB signaling in the psychopathology of this phenomenon is emphasized by the discovery that the presence of AAT repeats in the human *CNR1* gene encoding CB1R has been shown to be a risk factor for certain subtypes of schizophrenia (Ujike and Morita, 2004), and changes in CB1R expression have been observed in post-mortem schizophrenic brains (Dalton et al., 2011). Converging evidence from animal studies supports the idea that eCB signaling is particularly susceptible to insults during adolescence. In rodents, strong CB1R activation during adolescence usually produces permanent biochemical and behavioral changes, while adult brains are resistant to the same treatment (Quinn et al., 2008; Raver et al., 2013; Schneider et al., 2005; Schneider and Koch, 2003). In addition, neuroimaging studies in humans indicate that some mild cognitive deficits related to PFC pathophysiology are present before the onset of psychosis (Reichenberg et al., 2010), suggesting that acquired neural network vulnerability may be a critical step in the etiology of psychopathology. Our current studies demonstrate that adolescent CB1R hyperactivity in rodent brain triggers a sustained deficiency in presynaptic plasticity that is linked to the activity-dependent regulation of neural circuits. Such a deficit in synaptic activity could potentially lead to abnormalities in neural network homeostasis and, subsequently, to increased vulnerability of cortical circuits to dysfunction.

One possible explanation for the observed loss of eCB-LTD in WIN55-treated mice is a decreased level of CB1R expression. Changes in CB1R expression in the brain have been observed in adolescent rats treated with cannabinoids (Dalton and Zavitsanou, 2010; Rubino and Parolaro, 2014). CB1R expression is down-regulated by high levels of cannabinoids,

and this may contribute to the development of tolerance to the drug (Bedi et al., 2010; D'Souza et al., 2008; Gonzalez et al., 2005; Martini et al., 2010). Alternatively, attenuation of neurotransmission by CB1R receptor activation can be the result of desensitization, which involves uncoupling of CB1R from G-protein (Breivogel et al., 1999). Prolonged agonist activation desensitizes the responses of many G-protein-coupled receptors (GPCRs) (Gainetdinov et al., 2004). In general, GPCR desensitization occurs at a subsequent step after phosphorylation of the receptor by a G-protein coupled receptor kinase (GRK) and interaction of the phosphorylated receptor with an arrestin (Nguyen et al., 2012). Desensitization of CB1R involves GRK phosphorylation of the receptor at two serine residues, S426 and S430 (Daigle et al., 2008; Jin et al., 1999), a molecular event that contributes to cannabinoid tolerance (Morgan et al., 2014). Thus, the lack of eCB-LTD expression in our WIN55-treated mice could be a result of persistent desensitization of CB1Rs in response to higher levels of CB1R activation during adolescence. Unexpectedly, we also found a deficit in another form of presynaptic long-term depression at the L2/3→L5 synapse, mGluR2/3-LTD. Both CB1R and mGluR2/3 depend on the activity of G-protein-coupled receptors (GPCRs), and they share the same intracellular $G_{i/o}$ pathways and have been shown to actually occlude one another in some cases and to compensate for one another in other cases (Mato et al., 2008; Mato et al., 2005). While it cannot be ruled out that the LTD deficits we observed developed independently of each other, the observed deficits in two presynaptic forms of LTD could be a result of abnormal functioning of shared $G_{i/o}$ pathways. It is also possible that the observed deficits in WIN55-treated mice involve common downstream presynaptic signaling molecules that regulate presynaptic release, including adenylyl cyclase, protein kinase A, and possibly RIM1 α (Heifets and Castillo, 2009; Ohno-Shosaku et al., 2011). Further studies evaluating components of plasticity at the L2/3→L5 synapse in the mPFC are required to understand the events triggering an attenuation of both forms of LTD (i.e mGluR2/3-LTD and CB1R-LTD) in WIN55-treated mice.

Previous studies indicated that inhibition of synaptic transmission induced by agonist of group II mGluRs (i.e. mGluR2 and mGluR3) is mediated by presynaptic mGluR2 {Yokoi, 1996 #38537}{Kew, 2002 #42692}{Galici, 2006 #42687}{Benneyworth, 2007 #19958}{Galici, 2006 #42687}{Hermes, 2011 #42688}{Bradley, 2000 #42690;Johnson, 2011 #42689}. In addition, evidence suggests that that mGluR2/3-LTD in the mPFC involves a postsynaptic group II mGluR {Otani, 1999 #10237;Otani, 2002 #10231}. Recent studies with mGluR selective negative allosteric modulators in combination with mGluR2 and mGluR3 targeted knockout mice showed that mGluR2 mediates acute inhibition of synaptic transmission at glutamatergic L2/3→L5 synapses in the mPFC, whereas mGluR3 is required for induction of LTD at this synapse {Walker, 2015 #42664}. While induction of mGluR2/3-LTD revealed presynaptic component, mGluR2/3-LTD 60 min after induction exhibited lack of evidence for presynaptic component {Walker, 2015 #42664}. These data suggest that mGluR2/3-LTD expression may depend on a postsynaptic mechanism.

Accumulating evidence indicates that chronic adolescent, but not adult, exposure to cannabinoids produces permanent cognitive impairments in animal models (O'Shea et al., 2004; Quinn et al., 2008; Raver et al., 2013; Schneider et al., 2005; Schneider and Koch, 2003) and in humans (Meier et al., 2012; Solowij et al., 2002). Our current studies indicate

that behavioral changes triggered by adolescent CB1R stimulation coincides with biochemical and physiological changes in the rat brain that are linked to deficits in presynaptic forms of synaptic plasticity in an excitatory network. These data are consistent with recent findings demonstrating that THC exposure during adolescence disrupts the maturation of endocannabinoid system signaling and plasticity in the prefrontal cortex (Rubino et al., 2015). In addition, chronic exposure to the CB1R agonist WIN55,212-2 during adolescence, but not in adulthood, attenuates the power of cortical oscillations in the gamma frequency range in the mPFC in adult mice, a phenomenon that has been associated with cognitive decline (Raver et al., 2013). This finding is consistent with the results of studies involving marijuana users who initiated use as adolescents (Skosnik et al., 2012). These latter studies demonstrated that chronic cannabis exposure alters the ability to generate neural oscillations in the gamma range (Skosnik et al., 2012). Alterations in gamma oscillation have long been thought to be associated with schizophrenic etiology (Chen et al., 2014; Uhlhaas and Singer, 2013). It is noteworthy that developmental NMDAR hypofunction animal models for psychosis have also shown dysregulation in gamma oscillations in the cortex (Anderson et al., 2014; Hunt and Kasicki, 2013) and loss of eCB-LTD, while mGluR2/3-LTD was spared (Lovelace et al., 2014).

One limitation of this study is that we treated mice during adolescence with the commonly used synthetic CB1 agonist, WIN 55,212-2. This synthetic cannabinoid is a high efficacy agonist at CB1Rs and has a higher affinity than THC for this receptor. Thus, it is possible that the two compounds may differ in their effects. However, the synthetic compounds found in “spice” or “synthetic marijuana” (Castaneto et al., 2014) (which are synthetic cannabinoids marketed as alternatives to marijuana) generally are high efficacy agonists (Atwood et al., 2010; Atwood et al., 2011). In addition, studies involving participants who consumed high-potency skunk-like cannabis indicate that the risk for psychosis in cannabis users depends on the potency of the cannabis (Di Forti et al., 2015). Thus, adolescent WIN55 model used in the current studies may be a relevant model for chronic, high-potency cannabinoid consumption by adolescents.

In summary, an animal model of adolescent cannabinoid exposure in female rats shows a loss of activity- dependent presynaptic forms of plasticity. This type of retrograde endocannabinoid regulation appears to be a major regulator of neural network homeostasis and of the brain’s natural ability to adapt to a changing environment. Deficiency in a type of neural control that appears to function as an activity-dependent “brake” is likely to translate to maladaptations that underlie increased vulnerability to psychopathology.

ACKNOWLEDGMENTS

This work was supported by the UCR Collaborative Research Seed Grant (to EK), NIH/NIDA grants DA011322 and DA021696 (to KM) and Ford Fellowship (to PV).

References

Acheson SK, Moore NL, Kuhn CM, Wilson WA, Swartzwelder HS. The synthetic cannabinoid WIN 55212-2 differentially modulates thigmotaxis but not spatial learning in adolescent and adult animals. *Neurosci Lett.* 2011; 487:411–414. [PubMed: 21055447]

- Anderson PM, Pinault D, O'Brien TJ, Jones NC. Chronic administration of antipsychotics attenuates ongoing and ketamine-induced increases in cortical gamma oscillations. *Int J Neuropsychopharmacol.* 2014;1–10. [PubMed: 23953038]
- Arseneault L, Cannon M, Witton J, Murray RM. Causal association between cannabis and psychosis: examination of the evidence. *Br J Psychiatry.* 2004; 184:110–117. [PubMed: 14754822]
- Atwood BK, Huffman J, Straiker A, Mackie K. JWH018, a common constituent of 'Spice' herbal blends, is a potent and efficacious cannabinoid CB receptor agonist. *Br J Pharmacol.* 2010; 160:585–593. [PubMed: 20100276]
- Atwood BK, Lee D, Straiker A, Widlanski TS, Mackie K. CP47,497-C8 and JWH073, commonly found in 'Spice' herbal blends, are potent and efficacious CB(1) cannabinoid receptor agonists. *Eur J Pharmacol.* 2011; 659:139–145. [PubMed: 21333643]
- Bedi G, Foltin RW, Gunderson EW, Rabkin J, Hart CL, Comer SD, Vosburg SK, Haney M. Efficacy and tolerability of high-dose dronabinol maintenance in HIV-positive marijuana smokers: a controlled laboratory study. *Psychopharmacology (Berl).* 2010; 212:675–686. [PubMed: 20824270]
- Bodor AL, Katona I, Nyiri G, Mackie K, Ledent C, Hajos N, Freund TF. Endocannabinoid signaling in rat somatosensory cortex: laminar differences and involvement of specific interneuron types. *J Neurosci.* 2005; 25:6845–6856. [PubMed: 16033894]
- Breivogel CS, Childers SR, Deadwyler SA, Hampson RE, Vogt LJ, Sim-Selley LJ. Chronic delta9-tetrahydrocannabinol treatment produces a time-dependent loss of cannabinoid receptors and cannabinoid receptor-activated G proteins in rat brain. *J Neurochem.* 1999; 73:2447–2459. [PubMed: 10582605]
- Caspi A, Moffitt TE, Cannon M, McClay J, Murray R, Harrington H, Taylor A, Arseneault L, Williams B, Braithwaite A, Poulton R, Craig IW. Moderation of the effect of adolescent-onset cannabis use on adult psychosis by a functional polymorphism in the catechol-O-methyltransferase gene: longitudinal evidence of a gene X environment interaction. *Biol Psychiatry.* 2005; 57:1117–1127. [PubMed: 15866551]
- Castaneto MS, Gorelick DA, Desrosiers NA, Hartman RL, Pirard S, Huestis MA. Synthetic cannabinoids: epidemiology, pharmacodynamics, and clinical implications. *Drug Alcohol Depend.* 2014; 144:12–41. [PubMed: 25220897]
- Chen CM, Stanford AD, Mao X, Abi-Dargham A, Shungu DC, Lisanby SH, Schroeder CE, Kegeles LS. GABA level, gamma oscillation, and working memory performance in schizophrenia. *Neuroimage Clin.* 2014; 4:531–539. [PubMed: 24749063]
- Choi S, Lovinger DM. Decreased frequency but not amplitude of quantal synaptic responses associated with expression of corticostriatal long-term depression. *J Neurosci.* 1997a; 17:8613–8620. [PubMed: 9334432]
- Choi S, Lovinger DM. Decreased probability of neurotransmitter release underlies striatal long-term depression and postnatal development of corticostriatal synapses. *Proc Natl Acad Sci U S A.* 1997b; 94:2665–2670. [PubMed: 9122253]
- Crispim Junior CF, Pederiva CN, Bose RC, Garcia VA, Lino-de-Oliveira C, Marino-Neto J. ETHOWATCHER: validation of a tool for behavioral and video-tracking analysis in laboratory animals. *Comput Biol Med.* 2012; 42:257–264. [PubMed: 22204867]
- D'Souza DC, Ranganathan M, Braley G, Gueorguieva R, Zimolo Z, Cooper T, Perry E, Krystal J. Blunted psychotomimetic and amnesic effects of delta-9-tetrahydrocannabinol in frequent users of cannabis. *Neuropsychopharmacology.* 2008; 33:2505–2516. [PubMed: 18185500]
- Daigle TL, Kearn CS, Mackie K. Rapid CB1 cannabinoid receptor desensitization defines the time course of ERK1/2 MAP kinase signaling. *Neuropharmacology.* 2008; 54:36–44. [PubMed: 17681354]
- Dalton VS, Long LE, Weickert CS, Zavitsanou K. Paranoid schizophrenia is characterized by increased CB1 receptor binding in the dorsolateral prefrontal cortex. *Neuropsychopharmacology.* 2011; 36:1620–1630. [PubMed: 21471953]
- Dalton VS, Zavitsanou K. Cannabinoid effects on CB1 receptor density in the adolescent brain: An autoradiographic study using the synthetic cannabinoid HU210. *Synapse.* 2010; 64:845–854. [PubMed: 20842718]

- Di Forti M, Marconi A, Carra E, Fraietta S, Trotta A, Bonomo M, Bianconi F, Gardner-Sood P, O'Connor J, Russo M, Stilo SA, Marques TR, Mondelli V, Dazzan P, Pariante C, David AS, Gaughran F, Atakan Z, Iyegbe C, Powell J, Morgan C, Lynskey M, Murray RM. Proportion of patients in south London with first-episode psychosis attributable to use of high potency cannabis: a case-control study. *The Lancet Psychiatry*. 2015
- Fernandez-Espejo E, Viveros M-P, Núñez L, Ellenbroek BA, Rodriguez de Fonseca F. Role of cannabis and endocannabinoids in the genesis of schizophrenia. *Psychopharmacology*. 2009; 206:531–549. [PubMed: 19629449]
- Forbes NF, Carrick LA, McIntosh AM, Lawrie SM. Working memory in schizophrenia: a meta-analysis. *Psychol Med*. 2009; 39:889–905. [PubMed: 18945379]
- Fremeau RT Jr, Kam K, Qureshi T, Johnson J, Copenhagen DR, Storm-Mathisen J, Chaudhry FA, Nicoll RA, Edwards RH. Vesicular glutamate transporters 1 and 2 target to functionally distinct synaptic release sites. *Science*. 2004a; 304:1815–1819. [PubMed: 15118123]
- Fremeau RT Jr, Voglmaier S, Seal RP, Edwards RH. VGLUTs define subsets of excitatory neurons and suggest novel roles for glutamate. *Trends Neurosci*. 2004b; 27:98–103. [PubMed: 15102489]
- Freund TF, Katona I, Piomelli D. Role of endogenous cannabinoids in synaptic signaling. *Physiol Rev*. 2003; 83:1017–1066. [PubMed: 12843414]
- Gainetdinov RR, Premont RT, Bohn LM, Lefkowitz RJ, Caron MG. Desensitization of G protein-coupled receptors and neuronal functions. *Annu Rev Neurosci*. 2004; 27:107–144. [PubMed: 15217328]
- Gerdeman G, Lovinger DM. CB1 cannabinoid receptor inhibits synaptic release of glutamate in rat dorsolateral striatum. *J Neurophysiol*. 2001; 85:468–471. [PubMed: 11152748]
- Gerdeman GL, Lovinger DM. Emerging roles for endocannabinoids in long-term synaptic plasticity. *Br J Pharmacol*. 2003; 140:781–789. [PubMed: 14504143]
- Gogtay N, Giedd JN, Lusk L, Hayashi KM, Greenstein D, Vaituzis AC, Nugent TF 3rd, Herman DH, Clasen LS, Toga AW, Rapoport JL, Thompson PM. Dynamic mapping of human cortical development during childhood through early adulthood. *Proc Natl Acad Sci U S A*. 2004; 101:8174–8179. [PubMed: 15148381]
- Goldberg TE, Egan MF, Gscheidle T, Coppola R, Weickert T, Kolachana BS, Goldman D, Weinberger DR. Executive subprocesses in working memory: relationship to catechol-O-methyltransferase Val158Met genotype and schizophrenia. *Arch Gen Psychiatry*. 2003; 60:889–896. [PubMed: 12963670]
- Gonzalez S, Cebeira M, Fernandezruiz J. Cannabinoid tolerance and dependence: A review of studies in laboratory animals. *Pharmacology Biochemistry and Behavior*. 2005; 81:300–318.
- Harkany T, Mackie K, Doherty P. Wiring and firing neuronal networks: endocannabinoids take center stage. *Curr Opin Neurobiol*. 2008; 18:338–345. [PubMed: 18801434]
- Heifets BD, Castillo PE. Endocannabinoid Signaling and Long-Term Synaptic Plasticity. *Annual Review of Physiology*. 2009; 71:283–306.
- Hempel CM, Hartman KH, Wang XJ, Turrigiano GG, Nelson SB. Multiple forms of short-term plasticity at excitatory synapses in rat medial prefrontal cortex. *J Neurophysiol*. 2000; 83:3031–3041. [PubMed: 10805698]
- Hirsch JC, Crepel F. Use-dependent changes in synaptic efficacy in rat prefrontal neurons in vitro. *J Physiol*. 1990; 427:31–49. [PubMed: 2213602]
- Howlett AC, Barth F, Bonner TI, Cabral G, Casellas P, Devane WA, Felder CC, Herkenham M, Mackie K, Martin BR, Mechoulam R, Pertwee RG. International Union of Pharmacology. XXVII. Classification of cannabinoid receptors. *Pharmacol Rev*. 2002; 54:161–202. [PubMed: 12037135]
- Huang CC, Lo SW, Hsu KS. Presynaptic mechanisms underlying cannabinoid inhibition of excitatory synaptic transmission in rat striatal neurons. *J Physiol*. 2001; 532:731–748. [PubMed: 11313442]
- Hunt MJ, Kasicki S. A systematic review of the effects of NMDA receptor antagonists on oscillatory activity recorded in vivo. *J Psychopharmacol*. 2013; 27:972–986. [PubMed: 23863924]
- Jin W, Brown S, Roche JP, Hsieh C, Celver JP, Koo A, Chavkin C, Mackie K. Distinct domains of the CB1 cannabinoid receptor mediate desensitization and internalization. *J Neurosci*. 1999; 19:3773–3780. [PubMed: 10234009]

- Kasanetz F, Lafourcade M, Deroche-Gamonet V, Revest JM, Berson N, Balado E, Fiancette JF, Renault P, Piazza PV, Manzoni OJ. Prefrontal synaptic markers of cocaine addiction-like behavior in rats. *Mol Psychiatry*. 2013; 18:729–737. [PubMed: 22584869]
- Katona I, Sperlagh B, Sik A, Kafalvi A, Vizi ES, Mackie K, Freund TF. Presynaptically located CB1 cannabinoid receptors regulate GABA release from axon terminals of specific hippocampal interneurons. *J Neurosci*. 1999; 19:4544–4558. [PubMed: 10341254]
- Katona I, Urban GM, Wallace M, Ledent C, Jung KM, Piomelli D, Mackie K, Freund TF. Molecular composition of the endocannabinoid system at glutamatergic synapses. *J Neurosci*. 2006; 26:5628–5637. [PubMed: 16723519]
- Korzus E, Rosenfeld MG, Mayford M. CBP histone acetyltransferase activity is a critical component of memory consolidation. *Neuron*. 2004; 42:961–972. [PubMed: 15207240]
- Lafourcade M, Elezgarai I, Mato S, Bakiri Y, Grandes P, Manzoni OJ. Molecular components and functions of the endocannabinoid system in mouse prefrontal cortex. *PLoS ONE*. 2007; 2:e709. [PubMed: 17684555]
- Limback-Stokin K, Korzus E, Nagaoka-Yasuda R, Mayford M. Nuclear calcium/calmodulin regulates memory consolidation. *J Neurosci*. 2004; 24:10858–10867. [PubMed: 15574736]
- Long JZ, Li W, Booker L, Burston JJ, Kinsey SG, Schlosburg JE, Pavon FJ, Serrano AM, Selley DE, Parsons LH, Lichtman AH, Cravatt BF. Selective blockade of 2-arachidonoylglycerol hydrolysis produces cannabinoid behavioral effects. *Nat Chem Biol*. 2009; 5:37–44. [PubMed: 19029917]
- López-Gallardo M, López-Rodríguez AB, Llorente-Berzal Á, Rotllant D, Mackie K, Armario A, Nadal R, Viveros MP. Maternal deprivation and adolescent cannabinoid exposure impact hippocampal astrocytes, CB1 receptors and brain-derived neurotrophic factor in a sexually dimorphic fashion. *Neuroscience*. 2012; 204:90–103. [PubMed: 22001306]
- Lovelace JW, Vieira PA, Corches A, Mackie K, Korzus E. Impaired fear memory specificity associated with deficient endocannabinoid-dependent long-term plasticity. *Neuropsychopharmacology*. 2014; 39:1685–1693. [PubMed: 24457285]
- Lovinger DM. Presynaptic modulation by endocannabinoids. *Handb Exp Pharmacol*. 2008a; 184:435–477. [PubMed: 18064422]
- Lovinger DM. Presynaptic modulation by endocannabinoids. *Handb Exp Pharmacol*. 2008b:435–477. [PubMed: 18064422]
- Luzi S, Morrison PD, Powell J, di Forti M, Murray RM. What is the mechanism whereby cannabis use increases risk of psychosis? *Neurotox Res*. 2008; 14:105–112. [PubMed: 19073418]
- Mackie K. Signaling via CNS cannabinoid receptors. *Mol Cell Endocrinol*. 2008; 286:S60–65. [PubMed: 18336996]
- Makara JK, Mor M, Fegley D, Szabo SI, Kathuria S, Astarita G, Duranti A, Tontini A, Tarzia G, Rivara S, Freund TF, Piomelli D. Selective inhibition of 2-AG hydrolysis enhances endocannabinoid signaling in hippocampus. *Nat Neurosci*. 2005; 8:1139–1141. [PubMed: 16116451]
- Manrique-Garcia E, Zammit S, Dalman C, Hemmingsson T, Andreasson S, Allebeck P. Cannabis, schizophrenia and other non-affective psychoses: 35 years of follow-up of a population-based cohort. *Psychol Med*. 2011:1–8.
- Martini L, Thompson D, Kharazia V, Whistler JL. Differential Regulation of Behavioral Tolerance to WIN55,212-2 by GASPI1. *Neuropsychopharmacology*. 2010; 35:1363–1373. [PubMed: 20164830]
- Mato S, Chevalerey V, Robbe D, Pazos A, Castillo PE, Manzoni OJ. A single in-vivo exposure to delta 9THC blocks endocannabinoid-mediated synaptic plasticity. *Nat Neurosci*. 2004; 7:585–586. [PubMed: 15146190]
- Mato S, Lafourcade M, Robbe D, Bakiri Y, Manzoni OJ. Role of the cyclic-AMP/PKA cascade and of P/Q-type Ca⁺⁺ channels in endocannabinoid-mediated long-term depression in the nucleus accumbens. *Neuropharmacology*. 2008; 54:87–94. [PubMed: 17606273]
- Mato S, Robbe D, Puente N, Grandes P, Manzoni OJ. Presynaptic homeostatic plasticity rescues long-term depression after chronic Delta 9-tetrahydrocannabinol exposure. *J Neurosci*. 2005; 25:11619–11627. [PubMed: 16354920]
- Matsuda LA, Lolait SJ, Brownstein MJ, Young AC, Bonner TI. Structure of a cannabinoid receptor and functional expression of the cloned cDNA. *Nature*. 1990; 346:561–564. [PubMed: 2165569]

- Mechoulam R, Gaoni Y. A Total Synthesis of Δ^1 -Tetrahydrocannabinol, the Active Constituent of Hashish. *J Am Chem Soc.* 1965; 87:3273–3275. [PubMed: 14324315]
- Meier MH, Caspi A, Ambler A, Harrington H, Houts R, Keefe RS, McDonald K, Ward A, Poulton R, Moffitt TE. Persistent cannabis users show neuropsychological decline from childhood to midlife. *Proc Natl Acad Sci U S A.* 2012; 109:E2657–2664. [PubMed: 22927402]
- Morgan DJ, Davis BJ, Kearn CS, Marcus D, Cook AJ, Wager-Miller J, Straiker A, Myoga MH, Karduck J, Leishman E, Sim-Selley LJ, Czyzyk TA, Bradshaw HB, Selley DE, Mackie K. Mutation of putative GRK phosphorylation sites in the cannabinoid receptor 1 (CB1R) confers resistance to cannabinoid tolerance and hypersensitivity to cannabinoids in mice. *J Neurosci.* 2014; 34:5152–5163. [PubMed: 24719095]
- Morris SH, Knevet S, Lerner EG, Bindman LJ. Group I mGluR agonist DHPG facilitates the induction of LTP in rat prelimbic cortex in vitro. *J Neurophysiol.* 1999; 82:1927–1933. [PubMed: 10515982]
- Nguyen PT, Schmid CL, Raehal KM, Selley DE, Bohn LM, Sim-Selley LJ. beta-arrestin2 regulates cannabinoid CB1 receptor signaling and adaptation in a central nervous system region-dependent manner. *Biol Psychiatry.* 2012; 71:714–724. [PubMed: 22264443]
- Nyiri G, Cserep C, Szabadits E, Mackie K, Freund TF. CB1 cannabinoid receptors are enriched in the perisynaptic annulus and on preterminal segments of hippocampal GABAergic axons. *Neuroscience.* 2005; 136:811–822. [PubMed: 16344153]
- O'Shea M, Singh ME, McGregor IS, Mallet PE. Chronic cannabinoid exposure produces lasting memory impairment and increased anxiety in adolescent but not adult rats. *J Psychopharmacol.* 2004; 18:502–508. [PubMed: 15582916]
- Ohno-Shosaku T, Tanimura A, Hashimoto-dani Y, Kano M. Endocannabinoids and Retrograde Modulation of Synaptic Transmission. *The Neuroscientist.* 2011; 18:119–132. [PubMed: 21531987]
- Piomelli D. The molecular logic of endocannabinoid signalling. *Nat Rev Neurosci.* 2003; 4:873–884. [PubMed: 14595399]
- Quinn HR, Matsumoto I, Callaghan PD, Long LE, Arnold JC, Gunasekaran N, Thompson MR, Dawson B, Mallet PE, Kashem MA, Matsuda-Matsumoto H, Iwazaki T, McGregor IS. Adolescent rats find repeated Δ^9 -THC less aversive than adult rats but display greater residual cognitive deficits and changes in hippocampal protein expression following exposure. *Neuropsychopharmacology.* 2008; 33:1113–1126. [PubMed: 17581536]
- Raver SM, Haughwout SP, Keller A. Adolescent cannabinoid exposure permanently suppresses cortical oscillations in adult mice. *Neuropsychopharmacology.* 2013; 38:2338–2347. [PubMed: 23822952]
- Realini N, Vigano D, Guidali C, Zamberletti E, Rubino T, Parolaro D. Chronic URB597 treatment at adulthood reverted most depressive-like symptoms induced by adolescent exposure to THC in female rats. *Neuropharmacology.* 2011; 60:235–243. [PubMed: 20850463]
- Reichenberg A, Caspi A, Harrington H, Houts R, Keefe RS, Murray RM, Poulton R, Moffitt TE. Static and dynamic cognitive deficits in childhood preceding adult schizophrenia: a 30-year study. *Am J Psychiatry.* 2010; 167:160–169. [PubMed: 20048021]
- Robbe D, Alonso G, Chaumont S, Bockaert J, Manzoni OJ. Role of p/q- Ca^{2+} channels in metabotropic glutamate receptor 2/3-dependent presynaptic long-term depression at nucleus accumbens synapses. *J Neurosci.* 2002; 22:4346–4356. [PubMed: 12040040]
- Rubino T, Parolaro D. Cannabis abuse in adolescence and the risk of psychosis: a brief review of the preclinical evidence. *Prog Neuropsychopharmacol Biol Psychiatry.* 2014; 52:41–44. [PubMed: 23916409]
- Rubino T, Prini P, Piscitelli F, Zamberletti E, Trusel M, Melis M, Sgheddu C, Ligresti A, Tonini R, Di Marzo V, Parolaro D. Adolescent exposure to THC in female rats disrupts developmental changes in the prefrontal cortex. *Neurobiol Dis.* 2015; 73:60–69. [PubMed: 25281318]
- Rubino T, Realini N, Braida D, Alberio T, Capurro V, Vigano D, Guidali C, Sala M, Fasano M, Parolaro D. The depressive phenotype induced in adult female rats by adolescent exposure to THC is associated with cognitive impairment and altered neuroplasticity in the prefrontal cortex. *Neurotox Res.* 2009; 15:291–302. [PubMed: 19384563]

- Rubino T, Vigano D, Realini N, Guidali C, Braida D, Capurro V, Castiglioni C, Cherubino F, Romualdi P, Candeletti S, Sala M, Parolaro D. Chronic delta 9-tetrahydrocannabinol during adolescence provokes sex-dependent changes in the emotional profile in adult rats: behavioral and biochemical correlates. *Neuropsychopharmacology*. 2008; 33:2760–2771. [PubMed: 18172430]
- Rubino T, Zamberletti E, Parolaro D. Adolescent exposure to cannabis as a risk factor for psychiatric disorders. *Journal of Psychopharmacology*. 2011; 26:177–188. [PubMed: 21768160]
- Sales-Carbonell C, Rueda-Orozco PE, Soria-Gomez E, Buzsaki G, Marsicano G, Robbe D. Striatal GABAergic and cortical glutamatergic neurons mediate contrasting effects of cannabinoids on cortical network synchrony. *Proc Natl Acad Sci U S A*. 2013; 110:719–724. [PubMed: 23269835]
- Schneider M, Drews E, Koch M. Behavioral effects in adult rats of chronic prepubertal treatment with the cannabinoid receptor agonist WIN 55,212-2. *Behav Pharmacol*. 2005; 16:447–454. [PubMed: 16148450]
- Schneider M, Koch M. Chronic pubertal, but not adult chronic cannabinoid treatment impairs sensorimotor gating, recognition memory, and the performance in a progressive ratio task in adult rats. *Neuropsychopharmacology*. 2003; 28:1760–1769. [PubMed: 12888772]
- Skosnik PD, D'Souza DC, Steinmetz AB, Edwards CR, Vollmer JM, Hetrick WP, O'Donnell BF. The effect of chronic cannabinoids on broadband EEG neural oscillations in humans. *Neuropsychopharmacology*. 2012; 37:2184–2193. [PubMed: 22713908]
- Solowij N, Stephens RS, Roffman RA, Babor T, Kadden R, Miller M, Christiansen K, McRee B, Vendetti J. Cognitive functioning of long-term heavy cannabis users seeking treatment. *JAMA*. 2002; 287:1123–1131. [PubMed: 11879109]
- Stella N, Schweitzer P, Piomelli D. A second endogenous cannabinoid that modulates long-term potentiation. *Nature*. 1997; 388:773–778. [PubMed: 9285589]
- Straiker A, Hu SS, Long JZ, Arnold A, Wager-Miller J, Cravatt BF, Mackie K. Monoacylglycerol lipase limits the duration of endocannabinoid-mediated depolarization-induced suppression of excitation in autaptic hippocampal neurons. *Mol Pharmacol*. 2009; 76:1220–1227. [PubMed: 19767452]
- Tsou K, Mackie K, Sanudo-Pena MC, Walker JM. Cannabinoid CB1 receptors are localized primarily on cholecystokinin-containing GABAergic interneurons in the rat hippocampal formation. *Neuroscience*. 1999; 93:969–975. [PubMed: 10473261]
- Uhlhaas PJ, Singer W. High-frequency oscillations and the neurobiology of schizophrenia. *Dialogues Clin Neurosci*. 2013; 15:301–313. [PubMed: 24174902]
- Ujike H, Morita Y. New perspectives in the studies on endocannabinoid and cannabis: cannabinoid receptors and schizophrenia. *J Pharmacol Sci*. 2004; 96:376–381. [PubMed: 15613777]
- UNODC. World Drug Report. United Nations Publications; New York, NY: 2012. 2012.
- Wilson RI, Nicoll RA. Endogenous cannabinoids mediate retrograde signalling at hippocampal synapses. *Nature*. 2001; 410:588–592. [PubMed: 11279497]
- Zamberletti E, Beggiato S, Steardo L Jr, Prini P, Antonelli T, Ferraro L, Rubino T, Parolaro D. Alterations of prefrontal cortex GABAergic transmission in the complex psychotic-like phenotype induced by adolescent delta-9- tetrahydrocannabinol exposure in rats. *Neurobiol Dis*. 2014; 63:35–47. [PubMed: 24200867]

Highlights

- We used female mice to model adolescent cannabinoid exposure.
- We examine changes presynaptic long-term potentiation (LTP).
- Endocannabinoid-LTP and mGluR2/3-LTP are impaired in model for adolescent cannabinoid exposure.
- Adolescent CB1R agonist exposure triggers cognitive deficiency.

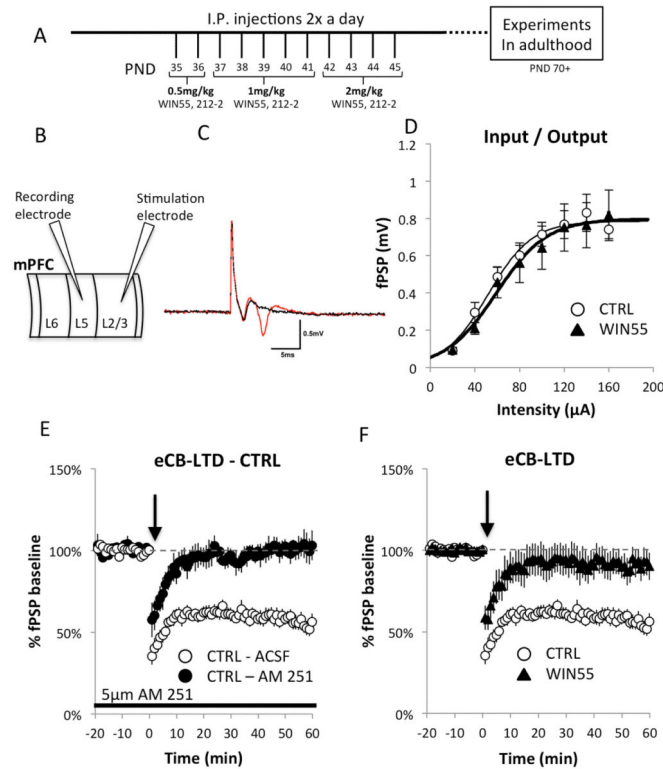


Figure 1.

Female rats receiving adolescent cannabinoids show a deficit in eCB-LTD, but preserved basal synaptic transmission.

(A) Injection protocol adapted from previous study (Rubino et al., 2008). Mice were injected twice a day during adolescence (PND35-45) with increasing doses of WIN55 and then allowed to mature to adulthood before experimental procedures. (B) Diagram showing the configuration of the recording and stimulation electrodes within the prelimbic region of the mPFC used in electrophysiological experiments to test synaptic activity at the L2/3→L5 synapse. (C) Application of DNQX shows the glutamatergic component of the fPSP. The red line is an average fPSP of 5 traces with only ACSF in the bath. After 5 min of bath application of 20 mM DNQX, another average of 5 traces was recorded (black line). Note that the fiber volley is spared while the fPSP is abolished under the DNQX condition (no picrotoxin present). (D) I/O curves were determined starting at 20 μ A stimulus intensity and increasing stimulation intensity until the amplitude measurements reached a plateau. No differences were detected using independent samples t-tests at any intensity measured (CTRL: n = 10; WIN55-treated: n = 11; all p-values > 0.05). A fitted curve for each group obtained using Boltzman's sigmoidal equations is also shown. Further detailed analysis of the I/O relationship was performed using different metrics obtained from the Boltzmann sigmoidal analysis to determine whether differences in the shape of the curves were present. A comparison of the means of individual Boltzmann fitted parameters revealed no differences between the WIN55-treated and control mice in the maximum asymptote (A2) p = 0.9130, in the center (x0) p = 0.1676, or in the time constant (dx) p = 0.2390. These thorough analyses of I/O relations at the L2/3→L5 synapse show that there are no differences between control and WIN55 mice in any of the tested characteristics of the I/O

curves. **(E)** The CTRL group showed robust expression of eCB-LTD at the L2/3→L5 synapse in the mPFC. eCB-LTD was induced at time 0 (black arrows) by application of a 10-Hz train for 10 min. LTD magnitude was estimated from fPSPs registered during the period 50-60 min after LTD induction and expressed as a percentage of baseline fPSP amplitudes. Bath application of 5 μ M AM 251 completely blocked LTD, indicating that this is an endocannabinoid-dependent form of LTD. **(F)** eCB-LTD was induced at time 0 (black arrow) with a 10-Hz train applied for 10 min using the previously described protocol (Lafourcade et al., 2007). LTD magnitude was estimated from fPSPs registered during the period 50-60 min after LTD induction as a percentage of baseline fPSP amplitudes. Compared with controls, WIN55-treated mice showed a strong deficit in eCB-LTD expression in response to the 10-Hz stimulation protocol (CTRL: $55.82\% \pm 4.08\%$, $n = 6$; WIN55-treated: $90.54\% \pm 7.63\%$, $n = 9$; $t_{(13)} = 3.469$, $p = 0.004$).

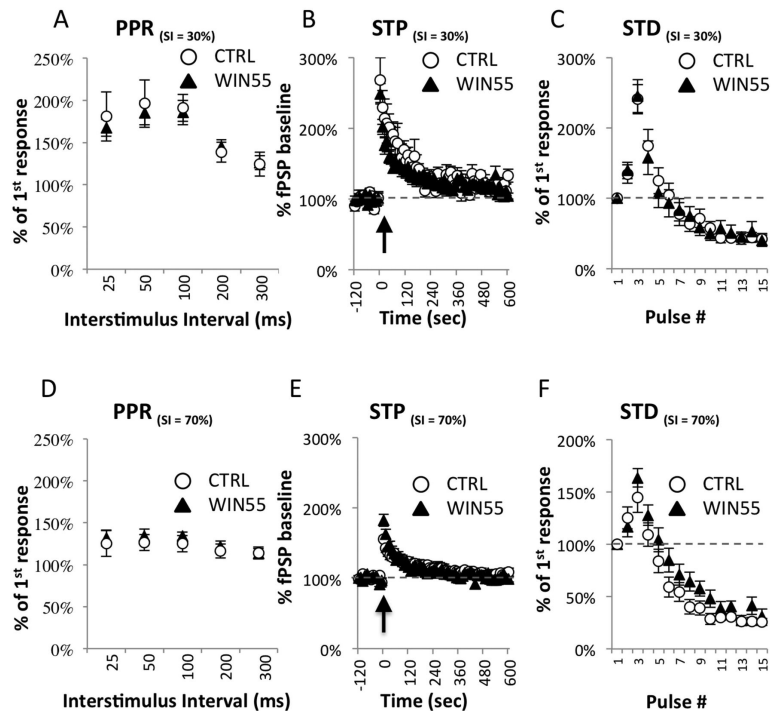


Figure 2.

Short-term plasticity at the L2/3→L5 synapse is unaffected in WIN55- treated mice. (A-C) Short-term measures of plasticity were measured at 30% stimulus intensity. (A) Paired-pulse ratios (PPR) were measured at the L2/3→L5 synapse at 5 different interstimulus intervals (25, 50, 100, 200, and 300 ms). No differences in mean PPR were observed between CTRL (n = 6) or WIN55-treated (n = 10) animals at any interval tested; all p-values > 0.05. (B) Short-term potentiation (STP) was induced with a brief train of 15 pulses delivered at 50 Hz at time 0 (indicated by a black arrow). RM-ANOVA between WIN55-treated (n = 10) and CTRL (n = 6) samples showed no time × treatment interaction ($F_{(1.6,21.3)} = 1.568$, $p = 0.232$). (C) Short-term depression (STD) was measured during the train used to simulate STP. Each response in the train was compared to the fPSP amplitude at baseline and plotted as a percentage. Depression across the train was observed in all groups, with facilitation being favored in the early portion of the train. RM-ANOVA revealed no significant pulse# × treatment interaction ($F_{(2.1, 28.7)} = 0.284$, $p = 0.760$). (D-F) Short-term measures of plasticity were also measured at 70% stimulus intensity. (D) PPRs were measured at 5 different inter-stimulus intervals (25, 50, 100, 200, and 300 ms). No differences in PPR at 70% stimulus intensity were observed between CTRL (n=6) and WIN55-treated (n=10) animals using independent samples t-tests; all p-values > 0.05. (E) RM-ANOVA on STP at 70% stimulus intensity between WIN55-treated (n=10) and CTRL (n=6) samples showed no time × treatment interaction ($F_{(2.1, 29.5)} = 1.501$, $p = 0.239$). (F) At 70% stimulus intensity, depression across the train was observed in both groups, with facilitation being favored in the early portion of the train but to a lesser extent than at 30% stimulus intensity. RM-ANOVA revealed no significant pulse# × treatment interaction $F_{(4,56)} = 2.154$, $p = 0.086$.

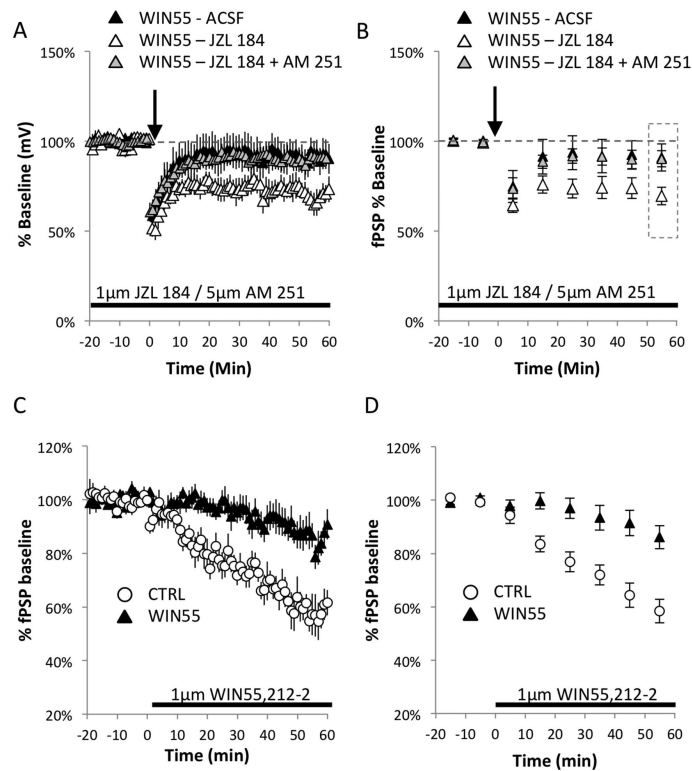


Figure 3.

Inhibition of 2-AG hydrolysis ameliorates the eCB-LTD deficiency at L2/3→L5 synapses.

(A) The WIN55-treated group showed no induction of LTD at the L2/3→L5 synapse in the mPFC. However, 10-min stimulation of slices from WIN55-treated mice at 10 Hz in the presence of 1 μM JZL 184 rescued the deficit (Wilcoxon test: WIN55-treated+JZL 184: $69.46\% \pm 4.90\%$, $Z = -2.366$, $n = 7$, $p = 0.018$). In addition, an attempt to rescue impaired eCB-LTD in the WIN55-treated mice with 1 μM JZL 184 failed in the presence of selective blocker of CB1R function AM 251 (5 μM). (B) The binned averages of 10 min time segments (calculated based on data in (A)) show distinct differences under all experimental conditions. Data were analyzed from the binned average time point in the rectangle marked during the last 10 min of recording. While WIN55-treated slices showed no induction of eCB-LTD, JZL 184 application to WIN55 slices enhanced LTD to control levels (Figure 1E), which failed in the presence of CB1R blocker AM 251 (C) CB1R function is reduced in WIN55-treated mice. The WIN55-treated group shows decreased functionality of CB1R at the L2/3→L5 synapse in the mPFC compared to control mice. After 20 min of baseline recording, continuous application of 1 μM WIN55,212-2, a CB1R agonist, caused a reduction of fPSP amplitude in the control group; this reduction was markedly dampened in the WIN55-treated mice. (D) Analysis of binned averages showed a markedly dampened effect in the WIN55-treated mice.

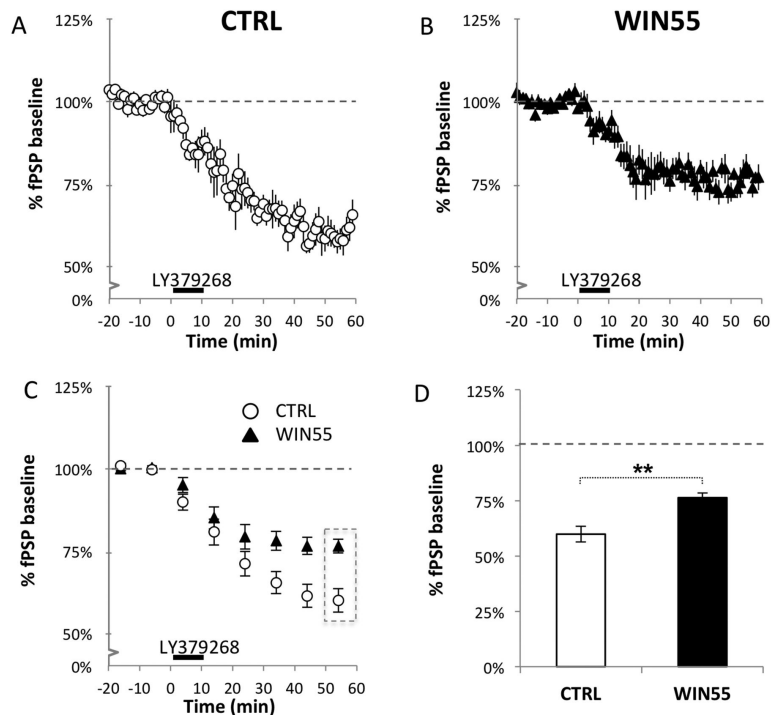


Figure 4. mGluR2/3-LTD at the L2/3→L5 synapse is suppressed in WIN55-treated mice. mGluR2/3-LTD in the L2/3→L5 pathway was induced at time 0 by a 10-minute bath application of 100 nM LY379268, a potent mGluR2/3 agonist. The CTRL group (**A**) showed significant expression of LTD, whereas LTD occurred to a lesser extent in the WIN55-treated group (**B**), suggesting that mGluR2/3-dependent LTD is altered in WIN55-treated mice. (**C**) Binned averages of activity taken every 10 min across time show significant divergence in mGluR2/3-LTD expression levels in WIN55-treated and control animals at the L2/3→L5 synapse; time \times treatment: $F_{(6,72)} = 3.715$, $p = 0.003$. (**D**) There is a significant difference in expression of mGluR2/3-LTD in control and WIN55-treated mice at 50-60 min (CTRL: $59.61\% \pm 3.27\%$, $n = 6$; WIN55-treated: $76.62\% \pm 2.06\%$, $n = 8$; $t_{(12)} = 4.625$, $p = 0.001$). These results suggest that treatment of mice with WIN55 during adolescence causes a disruption in the mGluR2/3 signaling pathway.

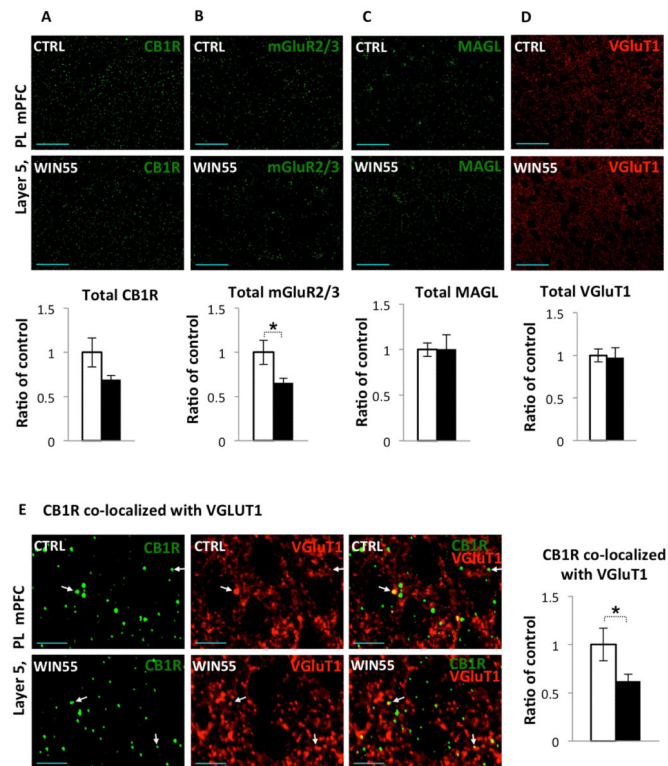


Figure 5.

CB1R and mGluR2/3 expression is reduced in WIN55-treated female mice. (A-D) Single optical section images were acquired at 40x magnification and a 1.5x Zoom from cortical layer 5 of the PL mPFC, top panels show images from control mice, middle panels show images from WIN55-treated mice (scale bar = 50 μ m) and lower panels give mean intensity of control (open bars) and WIN55-treated (filled bars) groups. (A) Mean intensity of the CB1R fluorescent signal in layer 5 of the PL mPFC of WIN55-treated mice was not significantly different from control mice ($p=0.0576$). (B) Mean intensity of mGluR2/3 signal in WIN55-treated mice showed a modest decrease in the mPFC (~35%, $p = 0.0417$). Mean intensity of MAGL (C) and VGLuT1 (D) staining in WIN55-treated mice were not different from those found in control animals ($p > 0.05$). (E) Single optical section images were acquired at 40x magnification and a 7x Zoom from cortical layer 5 of the PL mPFC. The first column (left) in green shows CB1R labeling, second column (middle) in red shows VGLuT1, and column 3 (right) shows the merged signals. Top panels show images from control mice and lower panels show images from WIN55-treated mice (scale bar = 10 μ m). WIN55-treated animals showed a modest decrease in CB1R co-localized with vGlut1 in L5 in the PL mPFC (~40%, $p = 0.0351$). White arrows indicate examples of CB1R co-localized with VGLuT1.

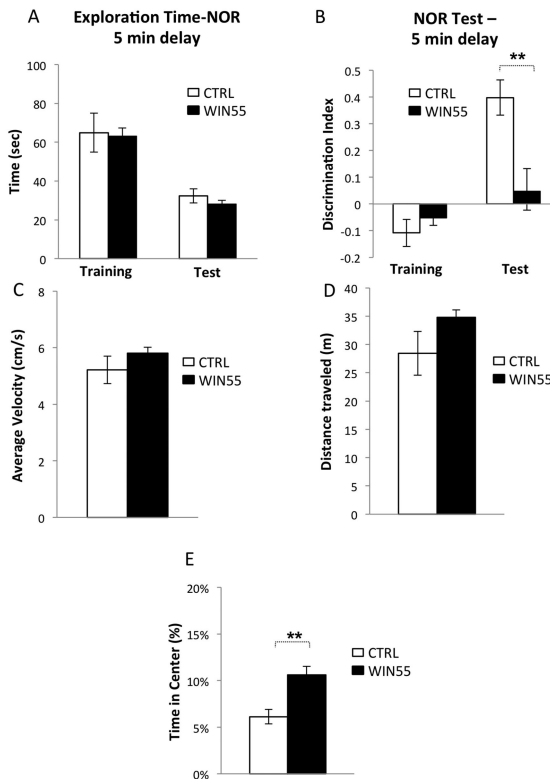


Figure 6.

WIN55 treatment during adolescence impairs performance on a novel object recognition task.

WIN55-treated and control mice were tested on a novel object recognition task with a 2-minute delay between the training and the testing phases. (A) Exploration time during training did not differ in the both groups. (B) While the two groups showed no difference in discrimination between objects during training, WIN55-treated mice failed to recognize the familiar object during the test phase. WIN55-treated mice show normal uninduced locomotor activity in the Open Field Activity test: average velocity (C) as well as total distance traveled (D) were unchanged. (E) However, WIN55-treated mice had increased center time in the Open Field Activity Test, consistent with decreased anxiety.